

# Cyclically Disentangled Feature Translation for Face Anti-spoofing

Haixiao Yue\*, Keyao Wang\*, Guosheng Zhang\*, Haocheng Feng, Junyu Han, Errui Ding, Jingdong Wang

Department of Computer Vision Technology(VIS), Baidu Inc.

{yuehaixiao, wangkeyao, zhangguosheng, fenghaocheng, hanjunyu, dingerrui}@baidu.com, wangjingdong@outlook.com

## Abstract

Current domain adaptation methods for face anti-spoofing leverage labeled source domain data and unlabeled target domain data to obtain a promising generalizable decision boundary. However, it is usually difficult for these methods to achieve a perfect domain-invariant liveness feature disentanglement, which may degrade the final classification performance by domain differences in illumination, face category, spoof type, etc. In this work, we tackle cross-scenario face anti-spoofing by proposing a novel domain adaptation method called cyclically disentangled feature translation network (CDFTN). Specifically, CDFTN generates pseudo-labeled samples that possess: 1) source domain-invariant liveness features and 2) target domain-specific content features, which are disentangled through domain adversarial training. A robust classifier is trained based on the synthetic pseudo-labeled images under the supervision of source domain labels. We further extend CDFTN for multi-target domain adaptation by leveraging data from more unlabeled target domains. Extensive experiments on several public datasets demonstrate that our proposed approach significantly outperforms the state of the art. Code and models are available at <https://github.com/vis-face/CDFTN>.

## Introduction

In recent years, face recognition has become a prominent technique for identity authentication and has been widely used in our lives. However, existing face recognition systems are vulnerable to face presentation attacks such as printed photos (i.e. print attack), digital images or videos (i.e. replay attack), and 3D facial masks (i.e. 3D mask attack), etc. In light of this urgency, the development of face anti-spoofing (FAS) technique has shown increasing significance in face recognition systems.

Various approaches have been proposed to train a generalizable classifier on different FAS scenarios. Most of existing solutions exploit multi-source domain generalization (DG) methods to learn a domain agnostic representation that aligns discriminative features on source domains, such that the model can generalize to the target domain without accessing its data. In practice, however, labeling the multiple

\*These authors contributed equally.

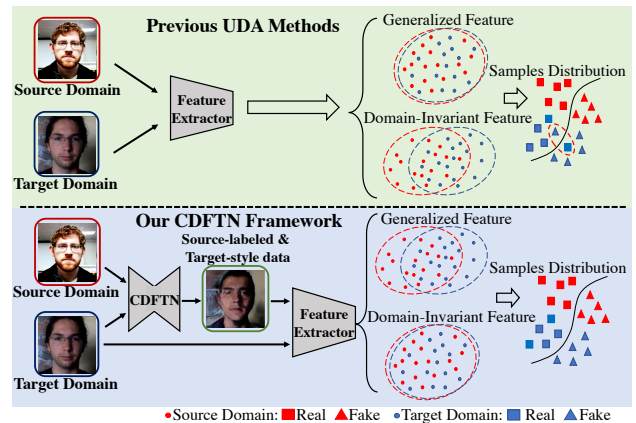


Figure 1: Framework comparison among our proposed method and previous UDA methods. The previous UDA methods translate generalized features which do not fit classification well. Our CDFTN method can disentangle and extract domain-invariant liveness features for better classification on the target domain.

source domains is time-consuming and laborious. Moreover, since we have access to plenty of unlabeled facial image data from an existing face recognition system, domain adaptation (DA) forms a natural learning framework for FAS. DA methods seek to aid cross-scenario FAS by extracting domain-indistinguishable feature representations from both labeled source data and unlabeled target data. Therefore, they can exploit rich information in the unlabeled target domain and obtain a more robust decision boundary.

On the FAS task, domain-invariant liveness feature extraction and translation are crucial to the final classification performance. Based on this thought, we assume that facial images in the FAS task could be mapped into two latent feature spaces: 1) a domain-invariant liveness feature space that represents the live-or-spoof attribute and 2) a domain-specific content feature space that represents face category, background environment, camera, and illumination, which is irrelevant to live-or-spoof classification. In this work, we propose a simple but effective cyclically disentangled feature translation network (CDFTN) to deal with the cross-scenario face anti-spoofing problem. Figure 1 presents how

to learn CDFTN with source and target domains.

In specific, CDFTN aims at generating cross-domain pseudo-labeled images, which is achieved by swapping the domain-invariant liveness features and the domain-specific content features from different domains. The labels of synthetic images are assigned to be the same as those of source domain images. To obtain disentangled representations along with effective generators, we employ GAN-like (Goodfellow et al. 2014) discriminators to conduct domain adversarial training. In addition, cyclic reconstruction and latent reconstruction are used to guarantee the effectiveness of disentangled feature translation. We finally train a robust classifier on the generated pseudo-labeled images and evaluate the trained classifier directly on the target dataset for testing. In contrast to existing DA-based FAS methods (Li et al. 2018; Wang et al. 2021a) that directly make decisions based on the exacted domain-invariant features, we instead use these features to synthesize training samples and obtain a discriminative classifier on synthetic pseudo-labeled training images.

Given the practical scenario that unlabeled target datasets from multiple domains are accessible, we extend our proposed method from single-source  $\rightarrow$  single-target feature translation to single-source  $\rightarrow$  multiple-targets translation. This extended network allows domain-invariant liveness features to transfer within multiple domains and generates pseudo-labeled images for each target domain. We finally train a robust classifier based on all pseudo-labeled images.

The contributions are summarized as follows:

- To tackle the cross-scenario FAS problem based on labeled source domain data and unlabeled target domain data, we propose to generate pseudo-labeled images to train a generalizable classifier.
- We design a novel feature translation framework using disentangled representation learning based on domain adversarial training; we also extend the framework from single-source  $\rightarrow$  single-target to single-source  $\rightarrow$  multiple-targets feature translation.
- Given unlabeled target domain data without other depth or temporal information, our approach achieves superior performance over the state-of-the-art methods.

## Related Works

### Face Anti-spoofing Methods

Traditional face anti-spoofing methods extract hand-crafted features such as LBP (Määttä, Hadid, and Pietikäinen 2011), HOG (Komulainen, Hadid, and Pietikäinen 2013), and SIFT (Patel, Han, and Jain 2016) to capture spoof patterns. With the recent development of deep learning, researchers use convolutional neural networks (CNN) to exploit deeper discriminative feature representations for face presentation attack detection (Atoum et al. 2017; Feng et al. 2020; Liu, Jourabloo, and Liu 2018; Yu et al. 2020a,b). CNN is used as a feature extractor for presentation attack detection, which is fine-tuned from ImageNet-pretrained ResNet (He et al. 2016) and VGG (Simonyan and Zisserman 2014). (Feng et al. 2020) proposes a residual-learning framework to learn

the discriminative spoof cues in the framework of anomaly detection. (Yu et al. 2020a) regards face anti-spoofing problem as a material recognition problem. (Yu et al. 2020b) proposes a framework based on central difference convolution. Several recent works (Feng et al. 2016; Wang et al. 2020b; Xu, Li, and Deng 2015) utilize LSTM or GRU to extract discriminative features in a stochastic manner for better classification performance. (Zhang et al. 2020b) trains the network in a unified multi-task framework. Although FAS has achieved great development in the past decade, the previously discussed methods only focus on a single domain and cannot generalize well on others.

### Unsupervised Domain Adaptation

Several recent domain generalization methods (Jia et al. 2020; Quan et al. 2021; Shao et al. 2019; Wang et al. 2020a; Liu et al. 2022; Wang et al. 2022) have achieved remarkable development on cross-domain FAS problem. Nevertheless, amount of unlabeled target data are available in some scenarios. But the data labeling work is laborious and time-consuming. Unsupervised domain adaptation (UDA) provides an alternative way by transferring knowledge from source domain to target domain. There are various types of proposed methods: (i) minimizing discrepancy between source and target domains sub-spaces (Gong et al. 2012; Long et al. 2013; Pan et al. 2010; Sun and Saenko 2015); (ii) domain confusion with adversarial approach (Donahue, Krähenbühl, and Darrell 2016; Kim et al. 2017; Tzeng et al. 2017); (iii) domain transformation with image-to-image translation (Lee et al. 2018; Yi et al. 2017; Zhu et al. 2017). However, there are only a few existing works focusing on FAS in the UDA framework, within which (Li et al. 2018) proposed a UDA framework for presentation-attack detection by minimizing Maximum Mean Discrepancy (MMD) (Gretton et al. 2012); (Jia et al. 2021; Wang et al. 2021a) proposed a UDA framework with adversarial training to improve the generalization capability of FAS model on target scenarios. (Wang et al. 2021b) proposed a self-domain adaptation framework to leverage the unlabeled test domain data at inference. However, it is usually difficult for these methods to achieve a perfect domain-invariant liveness feature disentanglement, which may degenerate the final classification performance.

### Disentangled Representation Learning

Deep neural networks are known to extract features where multiple hidden features are highly entangled (Peng, Li, and Saenko 2020; Zhuang et al. 2015). Disentangled representation learning focuses on extracting relevant features given a large variation of each dataset as well as irrelevant features that depict the relations between different domains. Recently, more and more state-of-the-art methods utilize generative adversarial networks (GAN) (Goodfellow et al. 2014) and variational autoencoders (VAE) (Kingma and Welling 2013) to learn disentangled representations given their success on image generation tasks. In the scenario of FAS, (Liu, Stehouwer, and Liu 2020) designs a novel adversarial learning framework to disentangle the spoof traces from input faces as a hierarchical combination of patterns at multiple

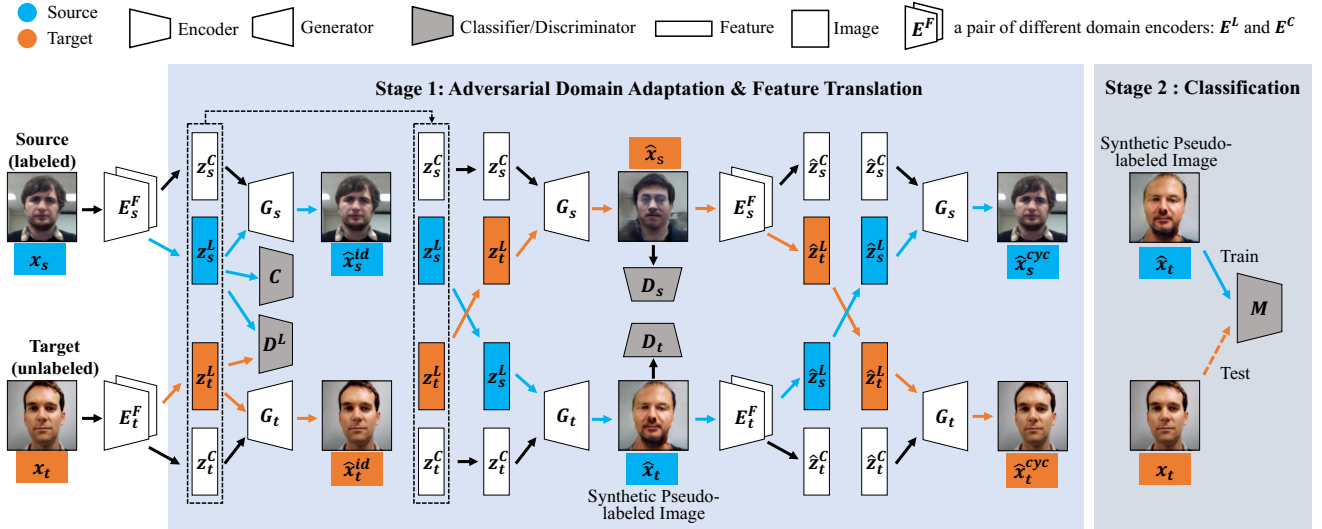


Figure 2: An overview of the model architecture. The network in Stage 1 visualizes the following functions of our model: 1) by applying a pair of different encoders (i.e.  $E^L$  and  $E^C$ ) in each domain, our model factorizes the liveness features and content features. 2) by using liveness discriminator  $D^L$  and classifier  $C$ , our model extracts domain-invariant liveness features through adversarial domain adaptation. 3) by exchanging  $z^L$  between domains, the generator  $G$  generates images based on cross-domain feature representations. Generated images in target domain  $\hat{x}_t$  would be passed to Stage 2 to obtain a domain-adapted classifier  $M$ .

scales. (Wang et al. 2020a) proposed a disentangled representation learning for cross-domain face presentation attack detection. (Zhang et al. 2020a) proposed a CNN architecture with the process of disentanglement and a combination of low-level and high-level supervision to improve generalization capabilities. Despite great achievement in FAS based on multi-level supervision, those methods cannot disentangle domain-specific and domain-invariant presentation attack representations thus would still overfit on training set.

## Proposed Method

The full network is illustrated in Figure 2. In this section, we introduce our problem statement and objectives, and then go through our proposed method in more details.

Suppose we have source dataset with  $n_s$  labeled examples  $\mathcal{S} = \{(x_s^i, y_s^i)\}_{i=1}^{n_s} \in X_s$ , where  $x_s^i \in \mathbb{R}^{H \times W \times 3}$  denotes the  $i^{th}$  source image and  $H, W$  stand for the height and width of  $x_s^i$ . Given the scenario of FAS,  $y_s^i$  is a one-hot vector with two elements corresponding to its label representing genuine or spoof. Similarly, we have a target dataset which includes  $n_t$  unlabeled examples  $\mathcal{T} = \{(x_t^i)\}_{i=1}^{n_t} \in X_t$  where  $x_t^i \in \mathbb{R}^{H \times W \times 3}$  denotes the  $i^{th}$  target image with the same size as  $x_s^i$ . Due to domain shift, the marginal distributions of source and target datasets are different, i.e.,  $P_S(X_s) \neq P_T(X_t)$ . The ultimate goal of our proposed method is to train a classifier that could effectively estimate  $P_T(Y_t|X_t)$  without the prior knowledge of  $P_T(Y_t)$ .

### Cross-Domain Feature Disentanglement

We first learn the common liveness-related features from source and target domains. Figure 2 presents our network.

Given the scenario of face anti-spoofing, we assume that both domains share common liveness properties despite the apparent differences between domains. We aim at mapping inputs from both domains into a common space. We first apply a pair of liveness encoder  $E_s^L$  and  $E_t^L$  to extract domain-invariant liveness features  $z_s^L$  and  $z_t^L$ , and a pair of content encoder  $E_s^C$  and  $E_t^C$  to extract domain-specific content features  $z_s^C$  and  $z_t^C$ . To determine the domain affiliation of extracted features  $z_s^L$  and  $z_t^L$ , we conduct domain adversarial training by applying a GAN-like (Goodfellow et al. 2014) discriminator  $D^L$ . We formulate the domain adversarial loss as follows:

$$\begin{aligned} \min_{E_s^L, E_t^L} \max_{D^L} \mathcal{L}_{D^L} = & \mathbb{E}_{x_s \sim P_S(x_s)} [\log D^L(E_s^L(x_s))] \\ & + \mathbb{E}_{x_t \sim P_T(x_t)} [\log(1 - D^L(E_t^L(x_t)))]. \end{aligned} \quad (1)$$

The discriminative property of encoded feature  $z_s^L$  is determined by labels of source domain. The cross-entropy loss of liveness feature from domain  $\mathcal{S}$  is formulated as follows:

$$\min_{E_s^L, C} \mathcal{L}_{cls^L} = -\mathbb{E}_{(x_s, y_s) \sim P_S(x_s, y_s)} [y_s \log C(E_s^L(x_s))], \quad (2)$$

where  $C$  is a binary classifier. A pair of decoders  $G_s$  and  $G_t$  is applied to reconstruct the extracted features back to original input image at the pixel level. We formulate reconstruction loss  $\mathcal{L}^{re}$  as:

$$\begin{aligned} \min_{G_d, E_d^f} \mathcal{L}^{re} = & \mathbb{E}_{x_s \sim P_S(x_s)} [\|G_s(E_s^L(x_s), E_s^C(x_s)) - x_s\|_1] \\ & + \mathbb{E}_{x_t \sim P_T(x_t)} [\|G_t(E_t^L(x_t), E_t^C(x_t)) - x_t\|_1], \end{aligned} \quad (3)$$

where  $d \in \{s, t\}$  and  $f \in \{L, C\}$ .

### Single-Target Feature Translation

Besides learning a common space for domain-invariant features, we also transfer them from labeled source domain to unlabeled target domain and use them to generate pseudo-labeled images. The architecture of feature translation framework is shown in the Figure 2. We further train a robust classifier on pseudo-labeled images and evaluate the classifier directly on original images in target domain. To generate ideal pseudo-labeled images, the extracted domain-invariant liveness features are swapped between domains and concatenated with corresponding domain-specific content features; then the concatenated feature is fed into  $G_s$  and  $G_t$  to construct fake images:  $\hat{x}_t = G_t(z_s^L, z_s^C)$ ,  $\hat{x}_s = G_s(z_t^L, z_t^C)$  and  $\hat{x}_t$  denotes pseudo-labeled images. To synthesize authenticate images, we further add a pair of discriminators  $D_s$  and  $D_t$  to differentiate between  $\hat{x}_s$  and  $x_s$ ,  $\hat{x}_t$  and  $x_t$ . The adversarial loss is formulated as:

$$\begin{aligned} \max_{D_s, D_t} \mathcal{L}_D^{adv} = & \mathbb{E}_{x_s \sim P_S(x_s)} [\log D_s(x_s) + \log(1 - D_s(\hat{x}_s))] \\ & + \mathbb{E}_{x_t \sim P_T(x_t)} [\log D_t(x_t) + \log(1 - D_t(\hat{x}_t))]. \end{aligned} \quad (4)$$

Inspired by (Zhu et al. 2017), the trained feature encoder and decoder functions should be able to bring  $x$  back to the original input, which is called *cycle consistency*. This statement holds an intuition that if the mapping functions are able to transfer features from domain  $\mathcal{S}$  to domain  $\mathcal{T}$ , then they are also expected to bring the same features back to the original domain. The cycle-consistency loss is formulated as:

$$\begin{aligned} \min_{G_d, E_d^f} \mathcal{L}^{cyc} = & \mathbb{E}_{x_s \sim P_S(x_s)} [\|G_s(E_t^L(\hat{x}_t), E_s^C(\hat{x}_s)) - x_s\|_1] \\ & + \mathbb{E}_{x_t \sim P_T(x_t)} [\|G_t(E_s^L(\hat{x}_s), E_t^C(\hat{x}_t)) - x_t\|_1]. \end{aligned} \quad (5)$$

Finally, to enforce the liveness features extracted from  $x_s(x_t)$  and  $\hat{x}_t(\hat{x}_s)$  to be unchanged after translation, we also apply the reconstruction loss between the domain-invariant liveness features as follows:

$$\begin{aligned} \min_{E_s^L, E_t^L} \mathcal{L}^{lat} = & \mathbb{E}_{x_s \sim P_S(x_s)} [\|E_s^L(\hat{x}_s) - E_t^L(x_t)\|_1] \\ & + \mathbb{E}_{x_t \sim P_T(x_t)} [\|E_t^L(\hat{x}_t) - E_s^L(x_s)\|_1]. \end{aligned} \quad (6)$$

### Full Objective Function

The whole network is trained step by step and we denote this training algorithm as **Single Source to Single Target** which

abbreviated as **SS2ST**. Optimization of proposed loss functions could be summarized as the following two stages:

**Stage 1** is shown in the first columns of Figure 2. We first simultaneously optimize Equations (1)-(6) to achieve both liveness feature domain adaptation and inter-domain translation. The objective function is:

$$\begin{aligned} \min_{G_d, E_d^f} \max_{D^L, D_d} \mathcal{L}^{\text{stage1}} \\ = \mathcal{L}_{cls^L} + \lambda_1 \mathcal{L}_{D^L} + \lambda_2 \mathcal{L}_D^{adv} + \lambda_3 \mathcal{L}^{re} + \lambda_4 \mathcal{L}^{cyc} + \lambda_5 \mathcal{L}^{lat}, \end{aligned} \quad (7)$$

where  $\{\lambda_k\}_{k=1}^5$  are hyper-parameters.

**Stage 2** is the training step as shown in the second columns of Figure 2. After Equation (7) converges, all parameters in CDFTN are fixed to generate pseudo-labeled images. The ultimate classifier (denoted as  $M$ ) is trained on generated image  $\hat{x}_t$ . We adopt two different architectures of the classifier for comparisons. For the first one, we select the LGSC (Feng et al. 2020) as the classifier since the method presents the best performance. The second one is the binary classifier of ResNet-18 (He et al. 2016). We denote these two different classifiers by L and R for short in the following (i.e., CDFTN-L and CDFTN-R). According to (Feng et al. 2020), the proposed loss consists of a auxiliary binary classification loss  $\mathcal{L}_a$ , a spoof cue  $L_1$  regression loss  $\mathcal{L}_r$ , and triplet loss  $\mathcal{L}_{tri}$ , while only binary classification loss  $\mathcal{L}_a$  is considered for ResNet-18(He et al. 2016). Therefore, the loss of stage 2 is defined as:

$$\min \mathcal{L}^{\text{stage2}} = \alpha_1 \mathcal{L}_a + \alpha_2 \mathcal{L}_r + \alpha_3 \mathcal{L}_{tri}, \quad (8)$$

where  $\{\alpha_k\}_{k=1}^3$  are hyper-parameters defined in (Feng et al. 2020) to control the relative importance of each objectives.

### Multi-Target Feature Translation

We propose to extend CDFTN to include multiple unlabeled target datasets. The network is presented in Figure 3. Suppose we have one labeled source domain and  $N$  unlabeled target domains, we use different liveness encoders  $E_s^L$  and  $\{E_{t_i}^L\}_{i=1}^N$  to extract liveness features  $z_s^L$  and  $\{z_{t_i}^L\}_{i=1}^N$  and apply  $N$  separate liveness discriminators  $\{D_{t_i}^L\}_{i=1}^N$  for domain adversarial training.

The extracted liveness features  $z^L$  are transferred via a forward loop from source domain  $\mathcal{S}$  to the target domain  $\mathcal{T}_1$ , from  $\mathcal{T}_1$  to target domain  $\mathcal{T}_2, \dots$ , and finally from target domain  $\mathcal{T}_N$  back to source domain  $\mathcal{S}$ . We use different content encoders  $E_s^C$  and  $\{E_{t_i}^C\}_{i=1}^N$  to extract domain-specific content features  $z_s^C$  and  $\{z_{t_i}^C\}_{i=1}^N$  and apply different decoders  $G_s$  and  $\{G_{t_i}\}_{i=1}^N$  in each domain to generate images  $\{\hat{x}_{t_i}\}_{i=1}^N$ . Similar to the training step as Figure 2 mentioned, we synthesize pseudo-labeled images  $\{\hat{x}_{t_i}^*\}_{i=1}^N$  and train a robust classifier  $M$  on all pseudo-labeled images. Similar to SS2ST, we denote this model extension module as **Single Source to Multiple Targets** short for **SS2MT**. The training steps are shown in Algorithm 1. When  $N = 1$ , 1 reduces to the SS2ST method.

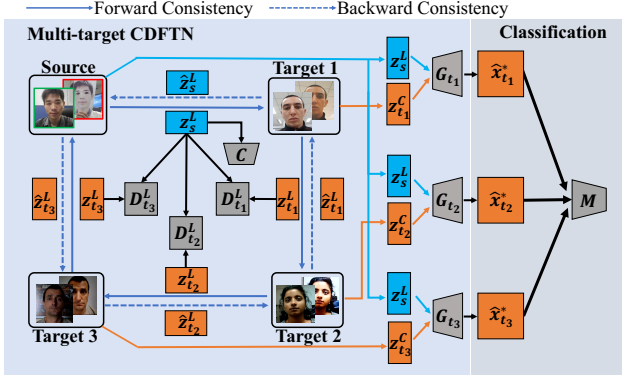


Figure 3: Network structure of multi-target translation where the model includes one labeled source domain and three unlabeled target domains corresponding to experimental settings. Forward consistency visualizes the path that  $z^L$  features are transferred through whereas backward consistency presents the path that  $z^L$  transferred back to the original domain. The synthetic pseudo-labeled images from multiple target domains ( $\hat{x}_{t_1}$ ,  $\hat{x}_{t_2}$ ,  $\hat{x}_{t_3}$ ) are combined to train a classifier  $M$ .

## Experiments

### Databases

We provide our evaluations on four publicly available databases for cross-domain FAS: CASIA-MFSD (Zhang et al. 2012) (C for short), Replay-Attack (Chingovska, Anjos, and Marcel 2012) (I for short), MSU-MFSD (Wen, Han, and Jain 2015) (M for short) and Oulu-NPU (Boulkenafet et al. 2017) (O for short). For SS2ST, we regard each dataset as a single domain to evaluate our model by selecting a source and target domain pair. The whole source domain dataset and the training set of target domain will be utilized in the training process. Therefore, in SS2ST we will experiment upon the following 12 scenarios:  $C \rightarrow I$ ,  $C \rightarrow M$ ,  $C \rightarrow O$ ,  $I \rightarrow C$ ,  $I \rightarrow M$ ,  $I \rightarrow O$ ,  $M \rightarrow C$ ,  $M \rightarrow I$ ,  $M \rightarrow O$ ,  $O \rightarrow C$ ,  $O \rightarrow I$  and  $O \rightarrow M$ . For SS2MT, among datasets C, I, M and O, we also select one as labeled source and the other three as unlabeled targets. Thus in SS2MT we have 4 scenarios:  $C \rightarrow I\&M\&O$ ,  $I \rightarrow C\&M\&O$ ,  $M \rightarrow C\&I\&O$  and  $O \rightarrow C\&I\&M$ .

### Evaluation Metrics

We use the Half Total Error Rate (HTER), which is the mean of False Rejection Rate (FRR) and False Acceptance Rate (FAR) for cross-domain FAS:

$$HTER = \frac{FRR + FAR}{2}. \quad (9)$$

We also export Area Under the Curve (AUC) for quantitative comparison between SS2ST and SS2MT.

### Implementation Details

In our experiment, we crop the human faces out of original images. For datasets that offer no face location ground truth, we use the Dlib (Kim et al. 2017) toolbox as the face detector. We resize our input image to  $224 \times 224 \times 3$ , where we

### Algorithm 1: Training Procedure of CDFTN

**Input:** Source  $\mathcal{S}$ ; Target  $\{\mathcal{T}_i\}_{i=1}^N$ ; Feature encoder  $E_s^L$ ,  $\{E_{t_i}^L\}_{i=1}^N$ ,  $E_s^C$ ,  $\{E_{t_i}^C\}_{i=1}^N$ ; Decoder  $G_s$ ,  $\{G_{t_i}\}_{i=1}^N$ ; Discriminator  $\{D_{t_i}^L\}_{i=1}^N$ ,  $D_s$ ,  $\{D_{t_i}^C\}_{i=1}^N$ ; Classifier  $C$ ,  $M$

**Output:** well-trained  $M^*$

**Notation:**  $\mathcal{D} = \{s, \{t_i\}_{i=1}^N\}$ ,  $\mathcal{F} = \{L, C\}$

```

1 while stage 1 not converged do
2   Random sample a mini-batch  $X_s$  from  $\mathcal{S}$  and
   mini-batches  $X_{t_1}, \dots, X_{t_N}$  from  $\mathcal{T}_1, \dots, \mathcal{T}_N$ ;
3   Adversarial domain adaptation;
4    $z_s^L = E_s^L(X_s)$ ,  $\{z_{t_i}^L = E_{t_i}^L(X_{t_i})\}_{i=1}^N$ ;
5   Update  $C$ ,  $E_s^L$  with (2);
6    $\forall d \in \mathcal{D}$ , update  $E_d^L$ ,  $\{D_{t_i}^L\}_{i=1}^N$  with (1);
7   Image generation;
8    $\hat{x}_s = G_s(z_s^L, z_s^C)$ ;
9    $\hat{x}_{t_1} = G_{t_1}(z_s^L, z_{t_1}^C)$ ,  $\{\hat{x}_{t_i} = G_{t_i}(z_{t_{i-1}}^L, z_{t_i}^C)\}_{i=2}^N$ ;
10   $\forall d \in \mathcal{D}$ , update  $E_d^C$ ,  $G_d$  with (4, 3),  $D_d$  with (4);
11  Cycle Consistency;
12   $\hat{x}_s^{cyc} = G_s(E_{t_1}^L(\hat{x}_{t_1}), E_s^C(\hat{x}_s))$ ;
13   $\{\hat{x}_{t_i}^{cyc} = G_{t_i}(E_{t_{i+1}}^L(\hat{x}_{t_{i+1}}), E_{t_i}^C(\hat{x}_{t_i}))\}_{i=1}^{N-1}$ ;
14   $\hat{x}_{t_N}^{cyc} = G_{t_N}(E_s^L(\hat{x}_s), E_{t_N}^C(\hat{x}_{t_N}))$ ;
15   $\forall d \in \mathcal{D}, \forall f \in \mathcal{F}$ , update  $E_d^f$ ,  $G_d$  with (5, 6)
16 end
17 while stage 2 not converged do
18    $\forall d \in \mathcal{D}, \forall f \in \mathcal{F}$ , fix  $E_d^f$ ,  $G_d$ ,  $D_d$  and  $\{D_{t_i}^L\}_{i=1}^N$ ;
19   Pseudo-labeled image synthesis;
20    $\{\hat{x}_{t_i}^* = G_{t_i}(z_s^L, z_{t_i}^C)\}_{i=1}^N$ ;
21   Classification;
22   Update  $M$  with (8)
23 end

```

extract the RGB channels of each image. Training examples are resampled to keep the live-spoof ratio to 1:1. We implement Equation (7) and Equation (8) separately. The Adam optimizer (Kingma and Ba 2014) is applied for both stages. In Stage 1, the learning rate is set as  $1 \times 10^{-3}$  and betas of optimizer are set to (0.5, 0.999); we choose values of  $\lambda_1$ ,  $\lambda_2$ ,  $\lambda_3$ ,  $\lambda_4$  as 1, 1, 10, 10, respectively; the batch size is set to be 2 and the training process lasts for 30 epochs. In Stage 2, we set  $\alpha_1$ ,  $\alpha_2$ ,  $\alpha_3$  to be the same as (Feng et al. 2020). During training, the batch size is set to be 32 and the classifier would be trained for 5 epochs.

### Comparison with State-of-Art-Methods

We compare our proposed method with other DA methods. The results are presented in Table 1. It can be found that the result of our proposed framework outstrips other methods. This is because our method encourages feature translation instead of simply domain adaptation that leverages target domain-specific features to obtain a robust and generalizable classifier. However, our method does not significantly improve cross-database testing performance when the

Method	C → I	C → M	C → O	I → C	I → M	I → O	M → C	M → I	M → O	O → C	O → I	O → M	Avg.
ADDA (Tzeng et al. 2017)	41.8	36.6	-	49.8	35.1	-	39.0	35.2	-	-	-	-	39.6
DRCN (Ghifary et al. 2016)	44.4	27.6	-	48.9	42.0	-	28.9	36.8	-	-	-	-	38.1
DupGAN (Hu et al. 2018)	42.4	33.4	-	46.5	36.2	-	27.1	35.4	-	-	-	-	36.8
KSA (Li et al. 2018)	39.3	15.1	-	12.3	33.3	-	9.1	34.9	-	-	-	-	24.0
DR-UDA (Wang et al. 2021a)	15.6	9.0	28.7	34.2	29.0	38.5	16.8	3.0	30.2	19.5	25.4	27.4	23.1
MDDR (Wang et al. 2020a)	26.1	20.2	<b>24.7</b>	39.2	23.2	33.6	34.3	8.7	31.7	21.8	27.6	22.0	26.1
ADA (Wang et al. 2019)	17.5	9.3	29.1	41.5	30.5	39.6	17.7	5.1	31.2	19.8	26.8	31.5	25.0
USDAN-Un (Jia et al. 2021)	16.0	9.2	-	30.2	25.8	-	13.3	3.4	-	-	-	-	16.3
<b>CDFTN-R</b>	5.4	14.4	32.5	<b>8.7</b>	12.9	<b>25.1</b>	13.5	5.6	28.2	<b>10.0</b>	<b>2.2</b>	7.1	13.8
<b>CDFTN-L</b>	<b>1.7</b>	<b>8.1</b>	29.9	11.9	<b>9.6</b>	29.9	<b>8.8</b>	<b>1.3</b>	<b>25.6</b>	19.1	5.8	<b>6.3</b>	<b>13.2</b>

Table 1: Cross-database testing results in comparison on four testing domains between our method and other methods. CDFTN-R and CDFTN-L denote using ResNet-18 and LGSC as the binary classifier respectively.

Method	SS2BT	SS2ST	SS2MT	
<b>C→I&amp;M&amp;O</b>	HTER(%)	15.9	13.3	<b>13.1</b>
	AUC(%)	89.5	90.8	<b>92.1</b>
<b>I→C&amp;M&amp;O</b>	HTER(%)	24.0	18.1	<b>17.0</b>
	AUC(%)	83.0	89.1	<b>90.2</b>
<b>M→C&amp;I&amp;O</b>	HTER(%)	19.6	11.6	<b>11.3</b>
	AUC(%)	88.2	93.2	<b>93.5</b>
<b>O→C&amp;I&amp;M</b>	HTER(%)	19.7	10.4	<b>7.8</b>
	AUC(%)	86.6	95.6	<b>97.4</b>

Table 2: Cross database testing results on the combination of three target domains. The results are reported as the average HTER and AUC scores. Specifically, the HTER scores of SS2ST are accordingly the arithmetic average of those shown in Table 1.

source domain is CASIA-MFSD and the target domain is Oulu-NPU. There two possible reasons for this result. (1) Oulu-NPU dataset is created with more presentation attack instruments (2 printers and 2 display devices vs. less in other datasets). (2) Oulu-NPU videos are recorded at Full HD resolution, i.e,  $1920 \times 1080$ , which is the resolution of high-quality videos of CASIA-MFSD. Therefore, resizing high-resolution images like Oulu-NPU will significantly blur the image and cause the performance drop.

### Effect of Multi-Target Feature Translation

We further conduct extensive experiment to illustrate the effect of model extension. In addition to SS2ST and SS2MT, we also conduct **Single Source to Blending Targets (SS2BT)**, which applies the same model as SS2ST, but the target domain is a mixture of multiple target domains. We report the average HTER and AUC score of the three target datasets and the results are shown in Table 2. It could be discovered that the results of SS2MT are significantly superior to those of SS2BT, which shows the single target liveness encoder is not capable of extracting a robust liveness feature for multiple sub-domains in a mixed target given the large variation between sub-domains. Therefore, regarding multiple sub-domains as separate individual domains, model extension will achieve better performance.

We also observe that the average HTER and AUC scores

of SS2MT are better than those of SS2ST. It implies that liveness feature of source domain in SS2MT contains more abundant information compared with SS2ST. In fact, SS2MT adapts liveness feature from source domain to multiple target domains, driving it to capture liveness information from more scenarios. In addition, SS2MT requires only one training cycle to obtain the results for multiple target domains.

### Ablation Study

We perform an ablation study to evaluate the contribution of each component of Equation (7) and compare the performance between two state-of-the-art binary classifiers: LGSC (Feng et al. 2020) and ResNet-18 (He et al. 2016). As also could be seen from the first five lines of Table 3, 1) we evaluate the performance of CDFTN w/o  $\mathcal{L}_{cls}^L$  (CDFTN without optimization of Equation (2)), and the performance is worse than full model. This is because optimization of Equation (2) drives  $z_s^L$  to be discriminative. 2) CDFTN w/o  $\mathcal{L}^{cyc}$  drops the optimization of cycle consistency loss, and its performance is worse than the full model. We consider that cycle consistency helps liveness feature transfer in a closed-loop instead of any random paths. 3). CDFTN w/o  $\mathcal{L}^{re}$  removes the contribution made by reconstruction loss, also resulting in worse performances, which illustrates that self-reconstruction loss is also crucial to regularize the feature mapping process. 4). CDFTN w/o  $\mathcal{L}^{lat}$  removes the contribution made by latent reconstruction loss, and the results are also worse than the full model; in fact, optimizing  $\mathcal{L}^{lat}$  ensures that liveness features extracted from original input and pseudo-labeled images are identical.

It could be discovered from Table 3 that all loss components are crucial to achieving the optimal solution. Comparing all components,  $\mathcal{L}^{re}$  is the most important as it aims at a robust reconstruction of original images during training;  $\mathcal{L}^{lat}$  is the second most important component as it enforces the liveness encoders to extract unchanged liveness features when encoding original images and pseudo-labeled images.

### Visualizations

Figure 5 presents our generated images (middle row) based on liveness feature of source domain (top row) and content feature of target domain (bottom row). We train classifier

Method	I → C	M → C	O → C	C → I	M → I	O → I	I → C	M → I	O → M	M Avg.
CDFTN-L w/o $\mathcal{L}_{cls}^L$	12.9	11.9	19.9	2.3	16.0	9.9	15.6	10.0	9.4	12.0
CDFTN-L w/o $\mathcal{L}^{cyc}$	12.4	14.4	23.8	1.9	4.9	6.2	11.1	15.2	9.3	11.0
CDFTN-L w/o $\mathcal{L}^{re}$	47.8	24.2	19.7	3.6	10.6	7.4	17.0	11.1	35.5	19.7
CDFTN-L w/o $\mathcal{L}^{lat}$	19.3	14.6	21.4	3.8	1.4	6.2	8.3	19.1	10.8	11.7
<b>CDFTN-L</b>	<b>11.9</b>	<b>8.8</b>	<b>19.1</b>	<b>1.7</b>	<b>1.3</b>	<b>5.8</b>	<b>8.1</b>	<b>9.6</b>	<b>6.3</b>	<b>8.1</b>

Table 3: Evaluation of each loss parts of our proposed framework on **C**, **I**, **O** and **M**.

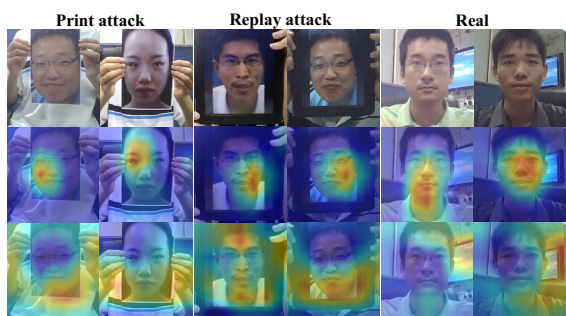


Figure 4: Grad-CAM (Selvaraju et al. 2017) visualizations of print attack, replay attack and real images by the ResNet-18 (middle row) and CDFTN-R method (bottom row) under the task **I** → **C**. Original images are shown in the top row.

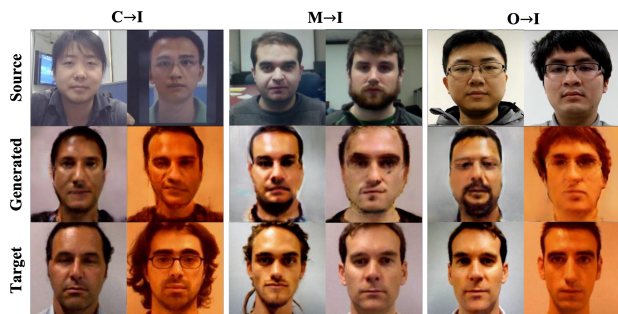
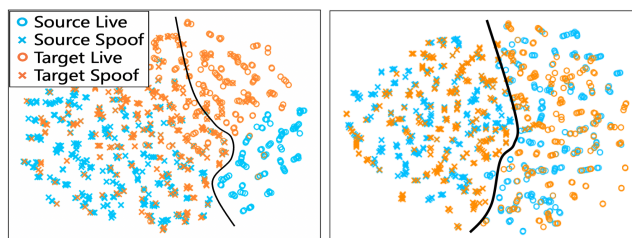


Figure 5: Visualizations of the generated images  $\hat{x}_t$  (middle row) based on the liveness features of source domain (top row) and content features of target domain (bottom row), i.e.  $\hat{x}_t = G_t(z_s^L, z_t^C)$ , given task **C** → **I**, **M** → **I** and **O** → **I**.

$M$  on the generated images. From the perspective of image-to-image translation, faces in different domains possess different identities and backgrounds, thus do not fulfill a strict bijection relationship and cycle consistency cannot be completely satisfied. Therefore, the generated images appear to be a random mixture of both domains and do not have decent quality. However, our main purpose in this work is to improve the performance of cross-domain face anti-spoofing and the current generated images are good enough to possess cross-domain feature representations.

As shown in Figure 4, we adopt Grad-CAM (Selvaraju et al. 2017) to show the class activation map (CAM) between the methods with and without CDFTN method. It shows that



(a) Before translation (b) After translation

Figure 6: The t-SNE (Maaten and Hinton 2008) visualization of feature distributions before and after feature translation upon task **M** → **I**. Blue and orange points represent source and target domain, respectively. Circle and cross points represent live and spoof samples, respectively.

the classifier based on ResNet-18 mostly focuses on the face region. However, our method CDFTN-R pays more attention to the region of hands and the edge of paper or screen.

### Qualitative Analysis

Considering the task of **M** → **I**, we visualize the feature distribution learned before and after feature translation to evaluate the optimization of domain divergence in Figure 6(a) and Figure 6(b), respectively. We randomly select 500 instances from each domains and plot t-SNE (Maaten and Hinton 2008) graphs. Comparing Figure 6(a) and Figure 6(b), we can discover that after adaptation, domain components are merged better than before, showing similar distributions between source and target domains. In addition, from the perspective of discriminative capability, a much clearer decision boundary is presented after feature translation.

### Conclusion

Cross-scenario face anti-spoofing remains a challenging task due to large variations in domain-specific features. In this work, we propose CDFTN to improve the current DA methods on FAS tasks. CDFTN achieves feature translation through swapping domain-invariant liveness features within domains. To achieve cyclic reconstruction, we propose to apply cycle consistency, self-reconstruction, and latent reconstruction modules. We train a classifier on pseudo-labeled images that generalizes well to target domain. Our experiments focus on evaluating the cross-database FAS performance and verify that our proposed method outperforms the state-of-the-art methods on various public datasets.

## References

- Atoum, Y.; Liu, Y.; Jourabloo, A.; and Liu, X. 2017. Face anti-spoofing using patch and depth-based CNNs. In *2017 IEEE International Joint Conference on Biometrics (IJCB)*, 319–328. IEEE.
- Boulkenafet, Z.; Komulainen, J.; Li, L.; Feng, X.; and Hadid, A. 2017. Oulu-npu: A mobile face presentation attack database with real-world variations. In *2017 12th IEEE International Conference on Automatic Face & Gesture Recognition (FG 2017)*, 612–618. IEEE.
- Chingovska, I.; Anjos, A.; and Marcel, S. 2012. On the effectiveness of local binary patterns in face anti-spoofing. In *2012 BIOSIG-proceedings of the international conference of biometrics special interest group (BIOSIG)*, 1–7. IEEE.
- Donahue, J.; Krähenbühl, P.; and Darrell, T. 2016. Adversarial feature learning. *arXiv preprint arXiv:1605.09782*.
- Feng, H.; Hong, Z.; Yue, H.; Chen, Y.; Wang, K.; Han, J.; Liu, J.; and Ding, E. 2020. Learning Generalized Spoof Cues for Face Anti-spoofing. *arXiv preprint arXiv:2005.03922*.
- Feng, L.; Po, L.-M.; Li, Y.; Xu, X.; Yuan, F.; Cheung, T. C.-H.; and Cheung, K.-W. 2016. Integration of image quality and motion cues for face anti-spoofing: A neural network approach. *Journal of Visual Communication and Image Representation*, 38: 451–460.
- Ghifary, M.; Kleijn, W. B.; Zhang, M.; Balduzzi, D.; and Li, W. 2016. Deep reconstruction-classification networks for unsupervised domain adaptation. In *European conference on computer vision (ECCV)*, 597–613. Springer.
- Gong, B.; Shi, Y.; Sha, F.; and Grauman, K. 2012. Geodesic flow kernel for unsupervised domain adaptation. In *2012 IEEE Conference on Computer Vision and Pattern Recognition*, 2066–2073. IEEE.
- Goodfellow, I.; Pouget-Abadie, J.; Mirza, M.; Xu, B.; Warde-Farley, D.; Ozair, S.; Courville, A.; and Bengio, Y. 2014. Generative Adversarial Nets. In Ghahramani, Z.; Welling, M.; Cortes, C.; Lawrence, N.; and Weinberger, K., eds., *Advances in Neural Information Processing Systems*, volume 27. Curran Associates, Inc.
- Gretton, A.; Borgwardt, K. M.; Rasch, M. J.; Schölkopf, B.; and Smola, A. 2012. A kernel two-sample test. *The Journal of Machine Learning Research*, 13(1): 723–773.
- He, K.; Zhang, X.; Ren, S.; and Sun, J. 2016. Deep residual learning for image recognition. In *Proceedings of the IEEE conference on computer vision and pattern recognition*, 770–778.
- Hu, L.; Kan, M.; Shan, S.; and Chen, X. 2018. Duplex generative adversarial network for unsupervised domain adaptation. In *Proceedings of the IEEE Conference on Computer Vision and Pattern Recognition*, 1498–1507.
- Jia, Y.; Zhang, J.; Shan, S.; and Chen, X. 2020. Single-side domain generalization for face anti-spoofing. In *Proceedings of the IEEE/CVF Conference on Computer Vision and Pattern Recognition*, 8484–8493.
- Jia, Y.; Zhang, J.; Shan, S.; and Chen, X. 2021. Unified unsupervised and semi-supervised domain adaptation network for cross-scenario face anti-spoofing. *Pattern Recognition*, 115: 107888.
- Kim, T.; Cha, M.; Kim, H.; Lee, J. K.; and Kim, J. 2017. Learning to discover cross-domain relations with generative adversarial networks. *arXiv preprint arXiv:1703.05192*.
- Kingma, D. P.; and Ba, J. 2014. Adam: A method for stochastic optimization. *arXiv preprint arXiv:1412.6980*.
- Kingma, D. P.; and Welling, M. 2013. Auto-encoding variational bayes. *arXiv preprint arXiv:1312.6114*.
- Komulainen, J.; Hadid, A.; and Pietikäinen, M. 2013. Context based face anti-spoofing. In *2013 IEEE Sixth International Conference on Biometrics: Theory, Applications and Systems (BTAS)*, 1–8. IEEE.
- Lee, H.-Y.; Tseng, H.-Y.; Huang, J.-B.; Singh, M.; and Yang, M.-H. 2018. Diverse image-to-image translation via disentangled representations. In *Proceedings of the European conference on computer vision (ECCV)*, 35–51.
- Li, H.; Li, W.; Cao, H.; Wang, S.; Huang, F.; and Kot, A. C. 2018. Unsupervised domain adaptation for face anti-spoofing. *IEEE Transactions on Information Forensics and Security*, 13(7): 1794–1809.
- Liu, S.; Lu, S.; Xu, H.; Yang, J.; Ding, S.; and Ma, L. 2022. Feature Generation and Hypothesis Verification for Reliable Face Anti-Spoofing. In *Thirty-Sixth AAAI Conference on Artificial Intelligence (AAAI)*.
- Liu, Y.; Jourabloo, A.; and Liu, X. 2018. Learning deep models for face anti-spoofing: Binary or auxiliary supervision. In *Proceedings of the IEEE conference on computer vision and pattern recognition*, 389–398.
- Liu, Y.; Stehouwer, J.; and Liu, X. 2020. On Disentangling Spoof Trace for Generic Face Anti-Spoofing. In *European Conference on Computer Vision (ECCV)*, 406–422. Springer.
- Long, M.; Wang, J.; Ding, G.; Sun, J.; and Yu, P. S. 2013. Transfer feature learning with joint distribution adaptation. In *Proceedings of the IEEE international conference on computer vision*, 2200–2207.
- Maaten, L. v. d.; and Hinton, G. 2008. Visualizing data using t-SNE. *Journal of machine learning research*, 9(Nov): 2579–2605.
- Määttä, J.; Hadid, A.; and Pietikäinen, M. 2011. Face spoofing detection from single images using micro-texture analysis. In *2011 international joint conference on Biometrics (IJCB)*, 1–7. IEEE.
- Pan, S. J.; Tsang, I. W.; Kwok, J. T.; and Yang, Q. 2010. Domain adaptation via transfer component analysis. *IEEE Transactions on Neural Networks*, 22(2): 199–210.
- Patel, K.; Han, H.; and Jain, A. K. 2016. Secure face unlock: Spoof detection on smartphones. *IEEE transactions on information forensics and security*, 11(10): 2268–2283.
- Peng, X.; Li, Y.; and Saenko, K. 2020. Domain2Vec: Domain Embedding for Unsupervised Domain Adaptation. *arXiv preprint arXiv:2007.09257*.
- Quan, R.; Wu, Y.; Yu, X.; and Yang, Y. 2021. Progressive Transfer Learning for Face Anti-Spoofing. *IEEE Transactions on Image Processing*, 30: 3946–3955.

- Selvaraju, R. R.; Cogswell, M.; Das, A.; Vedantam, R.; Parikh, D.; and Batra, D. 2017. Grad-CAM: Visual Explanations from Deep Networks via Gradient-Based Localization. In *2017 IEEE International Conference on Computer Vision (ICCV)*, 618–626.
- Shao, R.; Lan, X.; Li, J.; and Yuen, P. C. 2019. Multi-adversarial discriminative deep domain generalization for face presentation attack detection. In *Proceedings of the IEEE Conference on Computer Vision and Pattern Recognition*, 10023–10031.
- Simonyan, K.; and Zisserman, A. 2014. Very deep convolutional networks for large-scale image recognition. *arXiv preprint arXiv:1409.1556*.
- Sun, B.; and Saenko, K. 2015. Subspace Distribution Alignment for Unsupervised Domain Adaptation. In *BMVC*, volume 4, 24–1.
- Tzeng, E.; Hoffman, J.; Saenko, K.; and Darrell, T. 2017. Adversarial discriminative domain adaptation. In *Proceedings of the IEEE conference on computer vision and pattern recognition*, 7167–7176.
- Wang, G.; Han, H.; Shan, S.; and Chen, X. 2019. Improving cross-database face presentation attack detection via adversarial domain adaptation. In *2019 International Conference on Biometrics (ICB)*, 1–8. IEEE.
- Wang, G.; Han, H.; Shan, S.; and Chen, X. 2020a. Cross-domain Face Presentation Attack Detection via Multi-domain Disentangled Representation Learning. In *Proceedings of the IEEE/CVF Conference on Computer Vision and Pattern Recognition*, 6678–6687.
- Wang, G.; Han, H.; Shan, S.; and Chen, X. 2021a. Unsupervised adversarial domain adaptation for cross-domain face presentation attack detection. *IEEE Transactions on Information Forensics and Security*, 16: 56–69.
- Wang, J.; Zhang, J.; Bian, Y.; Cai, Y.; Wang, C.; and Pu, S. 2021b. Self-Domain Adaptation for Face Anti-Spoofing. *Proceedings of the AAAI Conference on Artificial Intelligence*, 35(4): 2746–2754.
- Wang, Z.; Wang, Z.; Yu, Z.; Deng, W.; Li, J.; Li, S.; and Wang, Z. 2022. Domain Generalization via Shuffled Style Assembly for Face Anti-Spoofing. In *CVPR*.
- Wang, Z.; Yu, Z.; Zhao, C.; Zhu, X.; Qin, Y.; Zhou, Q.; Zhou, F.; and Lei, Z. 2020b. Deep spatial gradient and temporal depth learning for face anti-spoofing. In *Proceedings of the IEEE/CVF Conference on Computer Vision and Pattern Recognition*, 5042–5051.
- Wen, D.; Han, H.; and Jain, A. K. 2015. Face spoof detection with image distortion analysis. *IEEE Transactions on Information Forensics and Security*, 10(4): 746–761.
- Xu, Z.; Li, S.; and Deng, W. 2015. Learning temporal features using LSTM-CNN architecture for face anti-spoofing. In *2015 3rd IAPR Asian Conference on Pattern Recognition (ACPR)*, 141–145. IEEE.
- Yi, Z.; Zhang, H.; Tan, P.; and Gong, M. 2017. Dualgan: Unsupervised dual learning for image-to-image translation. In *Proceedings of the IEEE international conference on computer vision*, 2849–2857.
- Yu, Z.; Li, X.; Niu, X.; Shi, J.; and Zhao, G. 2020a. Face anti-spoofing with human material perception. In *European Conference on Computer Vision (ECCV)*, 557–575. Springer.
- Yu, Z.; Zhao, C.; Wang, Z.; Qin, Y.; Su, Z.; Li, X.; Zhou, F.; and Zhao, G. 2020b. Searching central difference convolutional networks for face anti-spoofing. In *Proceedings of the IEEE/CVF Conference on Computer Vision and Pattern Recognition*, 5295–5305.
- Zhang, K.-Y.; Yao, T.; Zhang, J.; Tai, Y.; Ding, S.; Li, J.; Huang, F.; Song, H.; and Ma, L. 2020a. Face anti-spoofing via disentangled representation learning. In *European Conference on Computer Vision (ECCV)*, 641–657. Springer.
- Zhang, Y.; Yin, Z.; Li, Y.; Yin, G.; Yan, J.; Shao, J.; and Liu, Z. 2020b. CelebA-Spoof: Large-Scale Face Anti-Spoofing Dataset with Rich Annotations. In *European Conference on Computer Vision (ECCV)*.
- Zhang, Z.; Yan, J.; Liu, S.; Lei, Z.; Yi, D.; and Li, S. Z. 2012. A face antispoofing database with diverse attacks. In *2012 5th IAPR international conference on Biometrics (ICB)*, 26–31. IEEE.
- Zhu, J.-Y.; Park, T.; Isola, P.; and Efros, A. A. 2017. Unpaired image-to-image translation using cycle-consistent adversarial networks. In *Proceedings of the IEEE international conference on computer vision*, 2223–2232.
- Zhuang, F.; Cheng, X.; Luo, P.; Pan, S. J.; and He, Q. 2015. Supervised representation learning: Transfer learning with deep autoencoders. In *Twenty-Fourth International Joint Conference on Artificial Intelligence*.